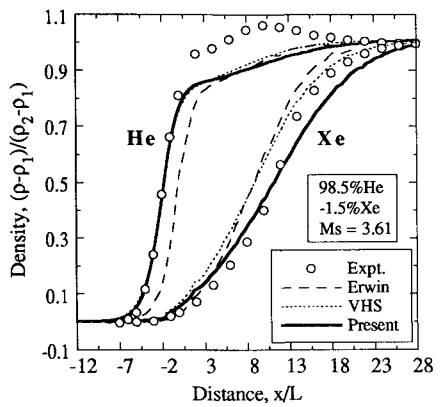

Fig. 2 Density profiles in a shock wave of 98.5% He, 1.5% Xe mixture.

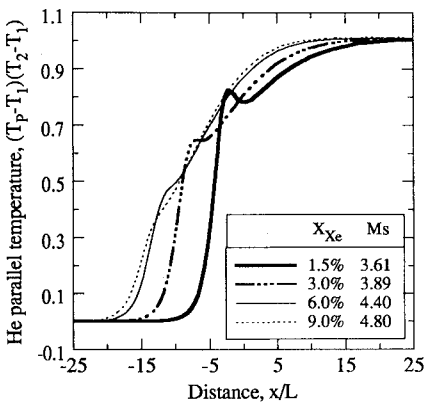

Fig. 3 Parallel temperature of helium in shock waves of He-Xe mixtures.

xenon and the preshock Mach number, respectively. Contrary to common expectations for a shock wave in a single component gas or a mixture composed of gases with a similar mass ratio, shock waves with less xenon mole fraction show a steeper parallel temperature profile in spite of higher preshock Mach numbers. An unusual aspect of the results in Fig. 3 is the hump in the helium parallel temperature profiles resulting from a strong species separation due to pressure diffusion of helium into the front part of the shock, which has never been reported either theoretically or experimentally. It is interesting to see that the location of the concavities preceded by the humps coincides with the location of the sharp inflection point in the density profiles shown in Figs. 1 and 2. The hump fades away when the mole fraction of xenon increases, as can be seen in the parallel temperature profiles for 6 and 9% xenon.

Conclusions

It has been shown that a realistic treatment of the molecular interactions of the colliding molecules can have a substantial effect in predicting the structure of a shock wave in disparate mass mixtures which involve large changes in mole fraction. The VDHS model was shown to offer better agreement with experimental data in predicting the separation of the species within helium-xenon shock waves. It is expected that the use of the VDHS model should offer more accurate results in predicting the separation of species in nonequilibrium flowfields of disparate mass mixtures which involve large changes in mole fraction, such as the flowfield in the plume and backflow regions of nuclear thermal rockets. The highly irregular behavior in the parallel temperature profile of the light species was observed in the DSMC simulation results, and this behavior has never been reported either theoretically or experimentally. This irregular behavior is thought to be physically more plausible than a smooth behavior, and future theoretical and experimental investigations of this phenomenon are recommended.

Acknowledgment

This work was sponsored by the NASA Lewis Research Center, Cleveland, Ohio, under Grant NCC 3-171. Robert M. Stubbs is the grant director.

References

[1]Bird, G. A., *Molecular Gas Dynamics*, Oxford Univ. Press, London, 1976.

[2]Bird, G. A., "Monte Carlo Simulation in an Engineering Context," *Rarefied Gas Dynamics*, edited by S. S. Fisher, Vol. 74, Pt. I, Progress in Astronautics and Aeronautics, AIAA, New York, 1981, pp. 239–255.

[3]Hash, D. B., and Hassan, H. A., "Monte-Carlo Simulation Using Attractive-Repulsive Potentials," Eighteenth International Symposium on Rarefied Gas Dynamics, Vancouver, Canada, July 1992.

[4]Koura, K., and Matsumoto, H., "Variable Soft Sphere Molecular Model for Inverse-Power-Law or Lennard-Jones Potential," *Physics of Fluids A*, Vol. 3, No. 10, 1991, pp. 2459–2465.

[5]Erwin, D. A., "Shock Wave in Mixtures: A Re-Examination," AIAA Paper 90-1750, June 1990.

[6]McDonald, J. D., "A Computationally Efficient Particle Simulation Method Suited to Vector Computer Architectures," Ph.D. Dissertation, Stanford Univ., Stanford, CA, Jan. 1990.

[7]Chung, C. H., De Witt, K. J., and Jeng, D. R., "New Approach in Direct-Simulation of Gas Mixtures," AIAA Paper 91-1343, June 1991.

[8]Gmurczyk, A. S., Tarczynski, M., and Walenta, Z. A., *Rarefied Gas Dynamics*, edited by R. Campargue, Commissiar a l'Energie Atomique, Paris, 1979, pp. 333–341.

[9]Piatkowski, T., "Application of the Modified BGK Equation to the Shock Wave Structures in Disparate Mass Mixtures," *Rarefied Gas Dynamics*, edited by R. Campargue, Commissiar a l'Energie Atomique, Paris, 1979, pp. 323–331.

[10]Chung, C. H., De Witt, K. J., Jeng, D. R., and Penko, P. F., "Internal Structure of Shock Waves in Disparate Mass Mixture," AIAA Paper 92-0496, Jan. 1992.

Use of Adaptive Finite Elements for Compressible Flow

Kevin L. Burton* and Darrell W. Pepper†
Advanced Projects Research, Inc., Moorpark, California 93021

Introduction

ADAPTIVE mesh refinement procedures with finite elements have been used for some time in computing compressible high-speed flows. Mesh refinement procedures for triangular finite element meshes were initially detailed by Zienkiewicz et al.[1] Applications of these procedures to compressible flow have been extensively demonstrated by Ramakrishnan et al.[2] Adaptive procedures for finite element meshes with quadrilateral elements are discussed in Oden et al.[3] and Shapiro and Murman.[4]

Received Jan. 25, 1992; revision received March 30, 1993; accepted for publication April 28, 1993. Copyright © 1993 by the American Institute of Aeronautics and Astronautics, Inc. All rights reserved.

*Engineer, 5301 North Commerce, Suite A. Member AIAA.

†Chairman of the Board, 5301 North Commerce, Suite A; currently Associate Professor, Department of Mechanical Engineering, University of Nevada—Las Vegas, Las Vegas, NV 89154. Senior Member AIAA.

Popular methods of mesh adaptation for finite element analysis are mesh movement or redistribution, mesh regeneration, and mesh enrichment. Mesh movement schemes hold the degrees of freedom (DOF) in a mesh constant, but move the mesh to capture regions of high gradients. Although easy to implement, the elements tend to become highly distorted. In mesh generation, a portion of the entire computational domain is regenerated when adaptation occurs. While this technique is time consuming and requires careful grid interpolation from old to new grids, the problem of grid distortion is significantly less.

Mesh enrichment consists of adding nodes or DOF in regions where solution gradients are high. Elements that lie in these regions are divided into smaller ones by a subdivision process. Both triangular and quadrilateral elements can be enriched by adding a central and/or midside node. These midside nodes are referred to as virtual or hanging nodes. The usual procedure for handling virtual nodes is to employ constraint equations that average nodal values of adjacent nodes to obtain the value at the virtual node. One way to avoid these unconnected nodes is to transition from a coarse quadrilateral mesh to a fine one using triangular elements.[2] This type of refinement removes the need for constraint equations, but adds complexity to the algorithm by combining quadrilaterals and triangles. A survey article by Berger[5] presents a good overview of grid enrichment methods. In this study, we examine the use of mesh enrichment using quadrilateral elements for two simple compressible flow problems.

Mesh Adaptation Procedure

The starting point of an adaptation procedure is a mesh coarse enough to allow rapid convergence, yet fine enough to allow the flow details to appear. An initial solution is then computed on the crude mesh. Refinement indicators are computed based on the solution with the initial mesh, and elements that need to be refined or unrefined are identified.

After the initial set of refinements and unrefinements are performed, the mesh is scanned for holes (an element with three or more of its faces subdivided). Each hole is then refined to reduce the number of virtual nodes (and hopefully increase solution accuracy). The process of eliminating holes will often create new holes, therefore, the process of refining holes is repeated until no holes are found.

After all the mesh changes have been made, the grid geometry is recalculated, the solution is interpolated onto the new grid, and the calculation procedure begun again. The entire procedure is repeated (or cycled) until a "converged" mesh is obtained, i.e., a mesh which no longer changes as the solution progresses. Cycling approximately 4–7 times is usually sufficient for the mesh to converge. The calculation procedure continues on the converged mesh until each of the dependent variables converge to a specified criterion.

Refinement Criteria

In order to decide which elements to refine or unrefine, some sort of adaptation parameter must be defined. For compressible flows, the density is typically used.[6] The adaptation parameter is calculated as follows:

1) In each element, calculate the absolute value of the first difference of density. For bilinear elements, the quantity used is $A_e = \max_{ij}|\rho_i - \rho_j|$.

2) Compute the mean and standard deviation of this quantity.

3) Normalize this quantity by subtracting the mean and dividing by the standard deviation.

The adaptive refinement procedure refines all elements that satisfy the criterion $A_e > \alpha$ and unrefines all elements that satisfy $A_e < \beta$, where α and β are preset threshold constants. The values of α and β are varied to cause more or less elements to be refined or unrefined, and are dependent on the flow features present. The values are usually determined experimentally and represent the optimum threshold values for the problem geometry.

When using quadrilateral elements, fluxes and the state vector at the virtual node are set equal to the average of the fluxes and state vectors at the corner nodes after each cycle. The time required in halving the virtual nodes is minimal compared to the complexity of mixing triangular and quadrilateral elements to avoid interface nodes. The procedure of setting the virtual node equal to the average of the state vectors at the corner nodes produces a consistent, conservative scheme.[6]

Results

Two inviscid compressible flow problems are analyzed using a simple Galerkin finite element approach[7] with mesh adaptation. A comparison solution is obtained by analytical analysis.

Converging Channel with 15-Deg Ramp

In the first problem, a planar 15-deg ramp is located on the lower wall of a two-dimensional channel. The inlet Mach number is 2.28. Based on one-dimensional ideal analysis, an oblique shock develops at an angle of 40 deg relative to the freestream. Downstream of the shock (region 2), $M_2 = 1.69$, $\rho_2/\rho_1 = 1.80$, and $P_2/P_1 = 2.34$.

A somewhat globally fine, uniform mesh is shown in Fig. 1a. Density contours for the Euler solution are presented in Fig. 1b. The profile shows a discontinuity at approximately 40 deg, in agreement with the ideal solution. However, the shock is diffused over many elements.

A very coarse mesh was initially used to obtain a representative bench mark for the adaptation process. The mesh provided a lower limit for the number of nodes required to allow flow features to develop. While the mesh allowed the shock to rapidly form, the shock became significantly smeared over many elements.

The refinement threshold value α was set equal to 0.8, and the unrefinement threshold value β was set equal to 0.2. Values for α ranged from 0.7–1.2, while β ranged from 0.0–0.4, without drastically altering the number of iterations required for convergence.

The number of levels of adaptation is crucial in obtaining an accurate solution with a minimal amount of computational time. Table 1 compares results for the globally fine mesh, coarse mesh, and three levels of adaptation with the analytical solution.

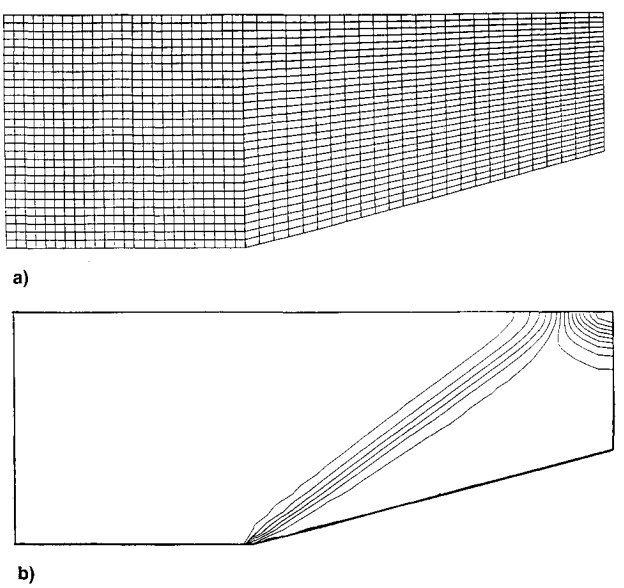

Fig. 1 Globally fine mesh and solution for converging channel: a) uniform mesh and b) density contours.

Table 1 Analytical/FEM ratios—converging channel with 15-deg ramp

Solution	Nodes	Element	CPU(s)	ts^a	M_2	ρ_2/ρ_1	P_2/P_1
Analytical					1.69	1.80	2.34
Globally fine mesh	1500	1421	1750	1145	1.75	1.86	2.38
Coarse mesh	240	207	244	250	1.84	1.76	2.78
One level of adaptation	382	324	425	1024	1.77	1.73	2.29
Two levels of adaptation	697	591	953	1695	1.74	1.86	2.37
Three levels of adaptation	1297	1092	1536	1832	1.68	1.84	2.37

[a]Steps to convergence.

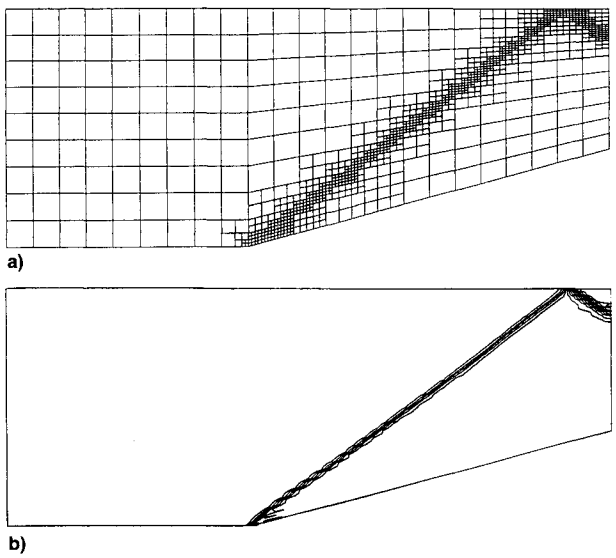

Fig. 2 Mesh and solution for converging channel-3 levels of adaptation: a) adapted mesh and b) density contours.

A mesh using one level of adaptation required three cycles before it converged. One level of adaptation was not enough to clearly capture and define the oblique shock wave. Two levels of mesh adaptation required five cycles before the mesh converged. Three levels of adaptation required six cycles before the mesh converged. The final mesh and density contours are presented in Figs. 2a and 2b. The density contours indicate that the shock has been well defined and restricted to an extremely thin band.

The number of iterations required for convergence is not a valid comparison because the meshes have different numbers of elements—the time required to perform an iteration varies from mesh to mesh. A CPU time comparison is also presented in Table 1. The CPU time required with two levels of adaptation is 45.5% less than that required using a globally fine mesh, which indicates that the use of mesh adaptation is clearly cost effective. Although the CPU time increases 38% when a third level of adaptation is used, the CPU time is still less than that for the globally fine mesh.

Converging Channel with Constant Area Extension

In the second problem, a constant area duct is added to the 15-deg converging channel. The inlet Mach number is 3.00. The complex geometry of this problem produces a shock train. The oblique shock formed at the front of the ramp intersects the upper surface and is reflected at an angle of 40.5 deg to the freestream. The reflected shock enters the constant area duct where it continues to reflect from the lower and upper surfaces of the duct, decreasing in strength and eventually becoming subsonic. Another complexity involved with this geometry is the interaction of the expansion wave and the reflected shock, which occurs at the start of the constant area duct.

The initial coarse mesh used for this problem consisted of 380 nodes and 333 elements. Two levels of mesh adaptation were deemed sufficient to capture the shock structure. The upper and lower refinement thresholds were set to 0.7 and 0.1, respectively. The converged mesh consisted of 1481 nodes and 1251 elements, and required 5731 iterations to converge. The final mesh and density contours for the solution are presented in Figs. 3a and 3b. An additional level of adaptation smoothed the contour plots, but did not significantly alter the numerical values.

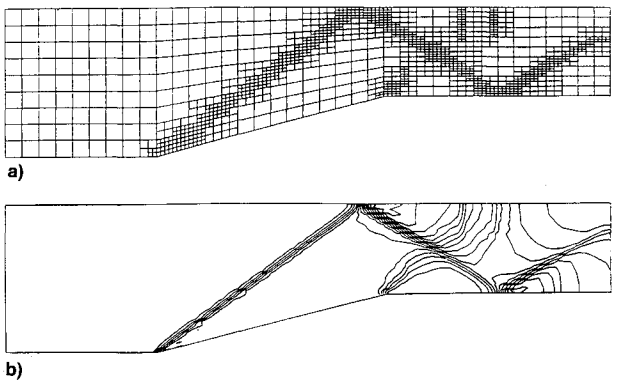

Fig. 3 Mesh and solution for converging channel with extension-2 levels of adaptation: a) adapted mesh and b) density contours.

Conclusions

The computational effort associated with mesh adaptation using quadrilateral finite elements has been examined using two simple compressible flow problems. The numerical results agree with analytical prediction and demonstrate the ability of the adaptation finite element method to model shocks and expansions with considerably good resolution at less computational effort than globally fine meshes.

One area which warrants further investigation is the need for improvement in the selection of indicators for use in adaptation, especially when shocks of different strength are involved. The algorithm is currently being used to examine compressible viscous flows as well as chemical effects.

References

[1]Zienkiewicz, O. C., Lohner, R., and Morgan, K., "High Speed Inviscid Compressible Flow by the Finite Element Method," *Mathematics of Finite Elements and Applications*, edited by J. R. Whiteman, Academic Press, New York, 1985, pp. 1–26.

[2]Ramakrishnan, R., Bey, K. S., and Thornton, E. A., "Adaptive Quadrilateral and Triangular Finite-Element Scheme for Compressible Flows," *AIAA Journal*, Vol. 28, No. 1, 1990, pp. 51–59.

[3]Shapiro, R. A., and Murman, E., "Adaptive Finite Element Methods for the Euler Equations," AIAA Paper 88-0034, Jan. 1988.

[4]Shapiro, R. A., "An Adaptive Finite Element Solution Algorithm for the Euler Equations," Ph.D. Dissertation, Dept. of Aeronautics and Astronautics, MIT Rept. CFDL-TR-88-7, Kansas City, MO, 1988.

[5]Berger, M. J., "Adaptive Finite Difference Methods in Fluid Dynamics," Courant Mathematics and Computing Lab., New York Univ., Technical Rept. DOE/ER/03077-277, New York, 1984.

[6]Oden, J. T., Strouboulis, T., and Devloo, Ph., "Adaptive Finite Element Methods for the Analysis of Inviscid Compressible Flow: Fast Refinement/Unrefinement and Moving Mesh Methods for Unstructured Meshes," *Computational Methods in Applied Mechanics and Engineering*, Vol. 59, No. 3, 1986, pp. 327–362.

[7]Pepper, D. W., and Humphrey, J. W., "A Modified Finite Element Method for CFD," AIAA Paper 89-0519, Jan. 1989.